Table 1. Summary of hSCF Tg NSG and non-Tg NSG recipients analyzed

				CBC at time of death					% chimerism at time of death			% of CD45+ in BM				% of CD33+ in BM			% of CD45+ in BM			% chimerism of erythroid cells in BM
Recipient ID	CB ID	Graft dose	Survival, wks	WBC, × 10^3/L	RBC, × 10^4/μL	Hemoglobin, g/dL	Hematocrit, %	Platelets, ×10^3/μL	PB	BM	Spleen	CD33+	CD3+	CD19+	CD3− CD56+	CD117+ CD203c+	HLA DR−	HLA DR+	CD117+ CD203c+	HLA DR−	HLA DR+	
N1-1	1	5000	21	1.1	500	10.0	35.0	550	75.5	93.3	95.3	31.1	1.2	50.2	0.3	0.9	51.5	47.6	0.3	16.0	14.8	NA
N1-2	1	5000	16	1.4	730	13.0	44.0	1100	42.6	76.1	72.9	35.2	0.1	54.8	0.4	0.7	39.6	59.7	0.2	13.9	21.0	NA
N1-3	1	5000	24	NA	NA	NA	NA	NA	20.7	12.6	4.4	32.9	3.8	60.7	0.0	4.4	37.9	57.7	1.0	12.5	19.0	3.1
S1-1	1	5000	23	4.1	220	6.7	15.6	150	99.1	99.7	94.4	77.2	24.5	19.2	0.5	3.9	80.6	15.5	3.0	62.2	11.9	NA
S1-2	1	5000	20	6.8	220	5.0	18.0	30	83.2	99.4	97.7	75.5	2.6	28.4	0.3	6.7	68.7	24.6	5.1	51.8	18.6	36.3
S1-3	1	5000	21	0.7	320	7.0	25.0	330	76.9	99.7	95.8	70.9	1.5	16.6	0.2	14.6	50.0	35.4	10.4	35.5	25.1	0.0
S1-4	1	500	26	0.5	150	3.0	11.0	250	30.7	97.0	86.3	69.0	2.0	47.5	0.1	6.9	68.6	24.5	4.8	47.3	16.9	NA
N2-1	2	10 000	35	0.8	390	8.0	30.0	110	31.7	54.9	87.1	50.3	21.8	25.8	2.4	19.1	7.4	73.5	9.6	3.7	37.0	11.5
S2-1	2	10 000	16	1.3	186	4.1	13.2	583	90.7	96.6	99.3	18.7	3.2	40.6	1.2	34.4	18.0	47.6	6.4	3.4	8.9	NA
S3-1	3	10 000	13	0.2	215	3.9	12.6	793	52.0	97.8	90.9	54.2	0.0	42.8	0.7	19.0	44.6	36.4	10.3	24.2	19.7	NA
S3-2	3	10 000	15	2.2	161	3.1	9.8	458	93.6	99.6	98.2	61.5	4.4	20.4	1.4	7.3	60.5	32.2	4.5	37.2	19.8	NA
S4-1	4	10 000	13	0.5	97	1.9	5.1	6	98.6	100.0	98.2	52.0	1.2	39.8	0.3	2.7	81.9	15.4	1.4	42.6	8.0	27.2
N5-1	5	12 000	35	3.1	310	7.0	25.0	550	6.8	36.8	48.9	29.9	17.5	41.9	NA	22.6	7.0	70.4	6.8	2.1	21.1	5.8
N6-1	6	14 000	23	2.1	520	10.0	34.0	620	57.6	65.0	83.6	29.3	17.6	43.1	1.6	3.3	45.1	51.6	1.0	13.2	15.1	7.4
N6-2	6	14 000	21	1.6	680	12.0	40.0	660	64.6	25.3	81.5	10.4	17.2	64.4	0.5	33.9	17.5	48.6	3.5	1.8	5.1	1.4
N6-3	6	14 000	24	2.3	490	10.0	33.0	80	73.8	71.8	92.8	18.5	13.9	51.1	0.8	10.6	8.5	81.4	2.0	1.6	15.1	12.8
S6-1	6	14 000	16	2.2	236	4.5	15.5	33	70.0	88.5	94.7	39.4	5.8	43.6	0.7	68.9	8.1	23.0	27.1	3.2	9.1	33.1
S6-2	6	14 000	14	4.6	270	6.0	21.0	108	85.4	90.0	95.2	33.3	11.6	46.8	0.9	36.5	16.0	47.5	12.2	5.3	15.8	5.8
S7-1	7	15 000	16	4.9	293	6.1	19.4	132	93.6	99.7	98.8	76.5	1.4	42.3	0.6	1.6	80.1	18.3	1.2	61.3	14.0	NA
S8-1	8	16 000	13	1.0	183	3.3	9.4	78	98.6	100.0	99.7	16.2	19.9	52.1	0.9	25.1	1.0	73.9	4.1	0.2	12.0	NA
S8-2	8	16 000	11	1.0	376	5.6	18.4	568	89.5	99.6	98.5	48.6	0.2	54.5	0.6	4.9	42.0	53.1	2.4	20.4	25.8	NA
N9-1	9	18 000	20	2.7	650	13.0	42.0	130	71.6	87.2	92.0	15.0	1.7	72.4	0.4	1.4	24.7	74.0	0.2	3.7	11.1	9.8
S9-1	9	18 000	16	1.4	164	3.4	10.6	80	90.4	99.9	97.0	51.4	0.2	35.1	0.2	2.4	54.9	42.7	1.2	28.2	21.9	25.5
N10-1	10	20 000	19	1.0	660	12.0	42.0	77	38.4	46.5	87.1	25.9	44.4	24.1	0.8	3.9	6.2	89.9	1.0	1.6	23.3	12.0
N10-2	10	20 000	14	NA	NA	NA	NA	NA	NA	NA	NA	NA	NA	NA	NA	NA	NA	NA	NA	NA	NA	NA
N10-3	10	20 000	12	NA	NA	NA	NA	NA	NA	NA	NA	NA	NA	NA	NA	NA	NA	NA	NA	NA	NA	NA
S10-1	10	20 000	19	2.5	292	6.1	20.9	6	95.5	99.7	97.3	42.3	14.4	35.5	0.9	5.7	28.8	65.5	2.4	12.2	27.7	4.3
S10-2	10	20 000	14	1.5	170	3.0	11.0	30	95.8	99.7	89.3	27.3	28.4	28.0	5.4	18.6	19.8	61.6	5.1	5.4	16.8	17.1
N11-1	11	36 000	20	25.1	470	9.0	31.0	240	84.1	70.7	94.0	19.5	5.9	63.6	0.7	3.8	17.8	78.4	0.7	3.5	15.3	42.3
S11-1	11	36 000	10	19.2	420	8.0	27.0	410	77.5	98.0	95.3	34.0	0.2	43.5	0.5	4.5	34.6	60.9	1.5	11.8	20.7	58.5
N12-1	12	53 000	8	NA	NA	NA	NA	NA	36.9	95.6	83.3	20.3	0.0	72.2	0.2	NA	NA	NA	NA	NA	NA	NA
S12-1	12	53 000	11	NA	NA	NA	NA	NA	100.0	100.0	99.9	43.5	6.5	39.1	1.5	NA	NA	NA	NA	NA	NA	NA
S12-2	12	53 000	8	NA	NA	NA	NA	NA	93.1	100.0	NA	65.6	0.2	13.2	NA	1.6	83.7	14.7	1.0	54.9	9.6	NA
S12-3	12	53 000	13	13.6	211	3.9	10.9	165	57.0	79.5	68.3	47.5	12.5	35.7	2.2	8.8	59.9	31.3	4.2	28.5	14.9	NA
N13-1	13	17 000	20	6.4	720	13.0	45.0	470	39.2	85.0	81.8	21.8	0.0	69.0	0.2	0.4	46.1	53.5	0.1	10.0	11.7	7.6
S13-1	13	17 000	20	2.8	290	7.0	27.0	510	74.9	93.7	94.5	38.1	6.0	47.8	0.4	26.6	31.3	42.1	10.1	11.9	16.0	48.4

A total of 21 human HSC-engrafted hSCFTg NSG (S) recipients and 15 human HSC-engrafted non-Tg NSG (N) recipients were created.
WBC indicates white blood cell count; RBC, red blood cell count; and NA, not applicable.

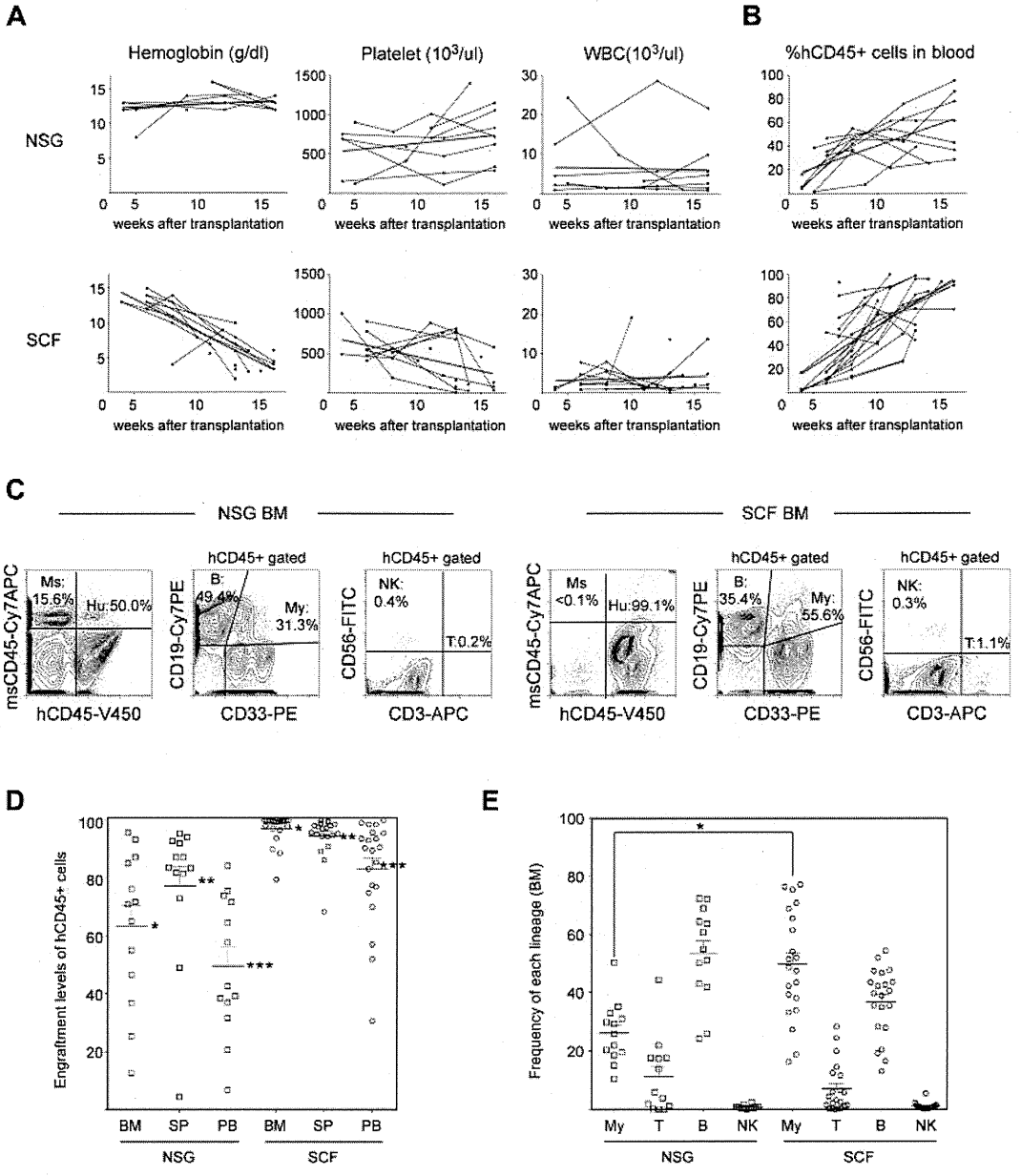

Figure 1. Human hematopoietic engraftment is enhanced in hSCF Tg NSG recipients. (A) hSCF Tg NSG recipients developed progressive anemia as evidenced by reduced hemoglobin concentration compared with non-Tg NSG mice transplanted with human HSCs from the same donor source. (B) Human CD45$^+$ chimerism was analyzed over time in PB of hSCF Tg and non-Tg NSG recipients. (C) Representative flow cytometric contour plots demonstrating the presence of human CD45$^+$ cells, CD19$^+$ B cells, CD33$^+$ myeloid cells, CD3$^+$ T cells, and CD56$^+$CD3$^-$ NK cells in recipient BM. (D) At the time of death, engraftment levels of human CD45$^+$ cells in the BM, spleen, and PB of hSCF Tg NSG recipients were significantly higher compared with non-Tg NSG controls (BM: hSCF Tg n = 21, non-Tg n = 13, $P < .0001$; spleen: hSCF Tg n = 21, non-Tg n = 13, $P = .0065$; PB: hSCF Tg n = 21, non-Tg n = 13, $P < .0001$). (E) In hSCF Tg NSG recipient BM, significantly greater human CD33$^+$ myeloid lineage development was observed (hSCF Tg n = 21, non-Tg n = 13, $P = .0002$).

Impaired mouse erythropoiesis in these engrafted hSCF Tg NSG mice was associated with rapid expansion of hCD45$^+$ hematopoietic cells compared with non-Tg NSG recipients (Figure 1B).

At 8 to 35 weeks after transplantation, individual hSCF Tg NSG recipients were analyzed to determine levels of reconstitution of human hematopoiesis and immunity in the BM, spleen, and PB. At the time of necropsy, we did not observe any gross macroscopic abnormalities in these recipients. We performed flow cytometric analysis to evaluate the engraftment levels of human CD45$^+$ cells (calculated as % hCD45$^+$ cells relative to total numbers of mouse and human CD45$^+$ cells in the nucleated cell gate). Engraftment levels of human CD45$^+$ leukocytes in the BM, spleen, and PB were significantly higher in hSCF Tg NSG recipients (mean ± SEM; 97.1% ± 1.1%, 94.5% ± 1.6%, and 83.1% ± 3.9%, respectively; n = 21) compared with engrafted non-Tg NSG recipients (63.1% ± 7.3%, 77.3% ± 6.9%, and 49.5% ± 6.5%, respectively; n = 13; $P < .0001$, $P = .0065$, and $P < .0001$ by 2-tailed t test, respectively; Figure 1C-D). Compared with enhanced engraftment of human leukocytes in the recipient BM, development of human erythroid precursors was not significantly different in hSCF Tg NSG recipients compared with non-Tg NSG recipients (hSCFTg: 25.6% ± 6.1%; n = 10 and non-Tg NSG controls: 11.4% ± 3.6%; n = 10; $P = .0601$; supplemental Figure 2). We next analyzed the development of human lymphoid and myeloid cells in the engrafted human CD45$^+$ hematopoietic cell populations by flow cytometry using monoclonal antibodies against hCD3, hCD19,

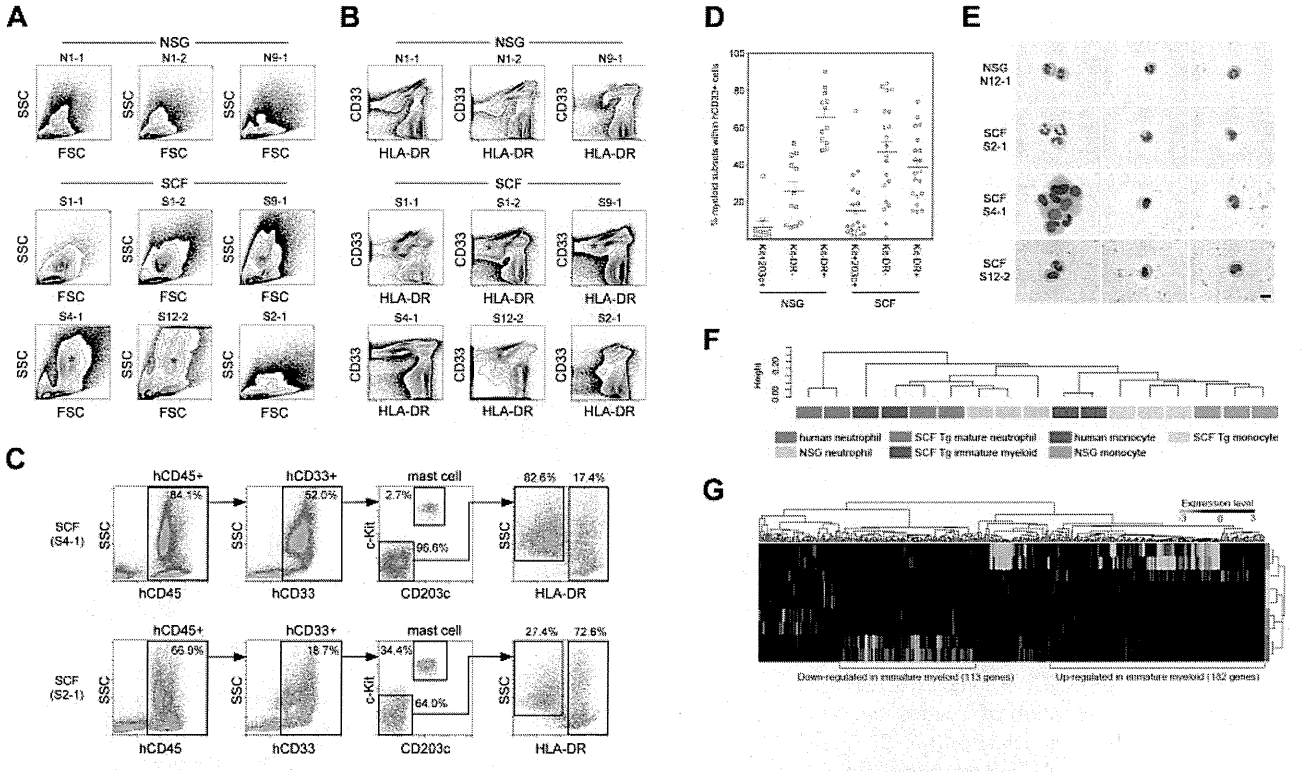

Figure 2. HLA-DR-negative human myeloid cells predominate in hSCF Tg NSG recipient BM. (A) Flow cytometric contour plots demonstrating FSC and SSC characteristics of 6 hSCF Tg NSG recipient BM (S1-1, S1-2, S9-1, S4-1, S12-2, and S2-1) and 3 non-Tg NSG recipient BM (N1-1, N1-2, and N9-1). Polymorphonuclear myeloid cells (red asterisks) are present at high frequencies in hSCF Tg NSG recipient BM. (B) Flow cytometry contour plots demonstrating hCD33 and HLA-DR expression in the same recipients as shown in panel A. Consistent with their FSC and SSC characteristics, hSCF Tg NSG recipient BM contained a prominent $CD33^+HLA\text{-}DR^-$ granulocyte population (red asterisks; N1-1, killed at 21 weeks; N1-2, killed at 16 weeks; N9-1, killed at 20 weeks; S1-1, killed at 23 weeks; S1-2, killed at 20 weeks; S9-1, killed at 16 weeks; S4-1, killed at 13 weeks; S12-2, killed at 8 weeks; and S2-1, killed at 16 weeks). (C) Representative flow cytometric scatter plots of hSCF Tg NSG recipient BM demonstrating the identification of human $c\text{-}Kit^+CD203c^+$ mast cells within the $hCD33^+$ fraction and $HLA\text{-}DR^-SSC^{high}$ granulocytes and $HLA\text{-}DR^+SSC^{low}$ APCs within the $c\text{-}Kit^-CD203c^-$ fraction (S4-1, killed at 13 weeks; and S2-1, killed at 16 weeks). (D) Frequencies of human $c\text{-}Kit^+CD203c^+$ mast cells, $CD33^+HLA\text{-}DR^-$ granulocytes, and $CD33^+HLA\text{-}DR^+$ APCs within the total $hCD45^+hCD33^+$ myeloid cell population in the BM of hSCF Tg and non-Tg NSG recipients. Numbers of cells in the granulocyte/neutrophil fraction were significantly higher in hSCF Tg NSG recipient BM (hSCF Tg n = 20, non-Tg n = 12, $P = .0001$). (E) $CD33^+HLA\text{-}DR^-$ cells from hSCF Tg and non-Tg NSG recipient BM were FACS-purified and examined by MGG staining. In 9 of 13 hSCF Tg recipients (S4-1 and S12-2 shown as representative), immature myeloid cells composed the majority of cells in this fraction. In 4 of 13 hSCF Tg recipients (S2-1 shown as representative) and 4 of 5 non-Tg NSG recipients (N12-1 shown as representative), mature neutrophils (band and segmented forms) were observed (N12-1, killed at 8 weeks; S2-1, killed at 16 weeks; S4-1, killed at 13 weeks; and S12-2, killed at 8 weeks). (F-G) Global transcriptional profiles of FACS-purified $CD33^+cKit^-CD203^-HLA\text{-}DR^-$ granulocytes and $CD33^+c\text{-}Kit^-CD203c^-HLA\text{-}DR^+CD14^+$ monocytes derived from hSCF Tg NSG and non-Tg NSG recipient BM as well as human $CD16^+$ neutrophils and $CD14^+$ monocytes were compared. (F) Unsupervised clustering for each group is shown. (G) The expression heatmap demonstrates genes that are significantly under- and over-represented in each population.

hCD56, and hCD33 along with anti–human and anti–mouse CD45 antibodies (Figure 1C,E). Although there was recipient-to-recipient variability, the frequency of human $CD33^+$ myeloid cells within the total human $CD45^+$ population was significantly higher in the hSCF Tg NSG recipient BM than in the non-Tg NSG recipient BM and constituted the majority of human hematopoietic cells (hSCF Tg: 49.7% ± 4.0%; n = 21 and non-Tg NSG controls: 26.2% ± 2.9%; n = 13; $P = .0002$ by 2-tailed t test). In contrast, in non-Tg NSG recipients, the majority of human hematopoietic cells in the BM were B cells (53.3% ± 4.5%; n = 13), consistent with previous reports.[5,9,20] These findings demonstrate that the expression of membrane-bound hSCF in BM microenvironment results in significantly more efficient engraftment of human HSCs as well as enhanced development of human $CD33^+$ myeloid cells from the engrafted human HSCs.

Human myeloid lineage development in hSCF Tg NSG recipients

Next, we examined the development of human myeloid subsets in the human membrane-bound SCF-expressing BM microenvironment. Flow cytometric scatter plots demonstrate the development of the SSC high granulocyte fraction in hSCF Tg NSG recipients, which correlate with $CD33^+HLA\text{-}DR^-$ cells (Figure 2A-B). To quantify the frequencies of different myeloid subsets in these recipients, we first identified $CD33^+c\text{-}Kit^+CD203c^+$ mature human mast cells among human $CD45^+$ cells. Next, we identified $CD33^+HLA\text{-}DR^-$ human granulocyte lineage cells and human $CD33^+HLA\text{-}DR^+$ antigen-presenting cells (APCs) among human $CD45^+$ cells excluding mature mast cells (Figure 2C).

In the hSCF Tg NSG recipient BM, there were increased percentages of $CD33^+HLA\text{-}DR^-$ granulocytes and decreased percentages of $CD33^+HLA\text{-}DR^+$ APCs compared with non-Tg NSG controls (hSCF Tg: 46.7% ± 5.9% and 38.3% ± 4.0%, respectively; n = 20 and non-Tg NSG controls: 25.8% ± 5.0% and 65.5% ± 4.1%, respectively; n = 12; $P = .0204$ and $P = .0001$ by 2-tailed t test, respectively; Figure 2D). In the BM of 11 of 20 hSCF Tg NSG recipients examined, $c\text{-}Kit^-CD203c^-HLA\text{-}DR^-$ SSC^{high} granulocytes accounted for the highest frequency of total human myeloid cells (Figure 2D; Table 1). To examine the morphologic features of the human granulocytes developing in the hSCF Tg recipients, we carried out May-Grünwald-Giemsa (MGG) staining using cytospin specimens of FACS-purified $CD33^+c\text{-}$

$Kit^-CD203c^-HLA\text{-}DR^-$ cells from BM of hSCF Tg and non-Tg NSG recipients. In 9 of 13 hSCF Tg recipient BM cells examined, the majority of myeloid cells showed the morphology of immature granulocytes with large nuclear-to-cytoplasmic ratio and nuclei with few lobulations, largely consisting of myelocytes and metamyelocytes (S4-1 and S12-2 shown as representative in Figure 2E). In 4 of 13 hSCF Tg recipients examined and in 4 of 5 non-Tg NSG recipients, mature segmented neutrophils were present in the sorted $CD33^+$c-$Kit^-CD203c^-HLA\text{-}DR^-$ granulocyte population (N12-1 and S2-1 shown as representative in Figure 2E). These findings indicate that both by quantitative and morphologic examinations, human granulocytic cells with various degrees of maturity predominate among the $CD33^+$ myeloid cells developing within the hSCF Tg NSG recipients. To examine the myeloid differentiation capacity of hematopoietic stem and progenitor populations in a functional manner, we performed a colony-forming cell assay using $CD34^+CD38^-$ and $CD34^+CD38^+$ cells derived from BM of hSCF Tg NSG recipients and non-Tg NSG recipients. In both cell populations, myeloid and erythroid colony formation were similar between hSCF Tg NSG and non-Tg NSG recipient BM (supplemental Figure 3).

We then analyzed global transcriptional profiles of $CD33^+HLA\text{-}DR^-$c-$Kit^-CD203c^-$ granulocytes from hSCF Tg NSG recipient BM (n = 4), non-Tg NSG recipient BM (n = 3), and primary human BM (n = 2). Additional control samples included BM monocytes from hSCF Tg recipients (n = 3), non-Tg NSG recipient BM monocytes (n = 3), and primary human BM monocytes (n = 2). Unsupervised clustering demonstrated a clear segregation of transcriptional profiles between granulocytes and monocytes regardless of the source. This suggests that human granulocytes and monocytes in humanized mouse undergo a distinct differentiation process similar to their counterparts in human BM (Figure 2F). We next examined whether there were any differences in gene expression within 3 distinct granulocyte sources (hSCF Tg recipient BM, non-Tg NSG recipient BM, and primary human BM neutrophils; Figure 2G). As seen in the heatmap representation, we found clusters of genes differentially transcribed in the distinct sources of granulocytes (Figure 2G). Multiple genes associated with transcriptional regulation were included in the genes upregulated in human immature granulocytes derived from the BM of hSCF Tg NSG mice, suggesting that these cells are more actively cycling and proliferating compared with mature granulocytes from the BM of hSCF Tg NSG and non-Tg NSG mice and primary human BM neutrophils (Figure 2G; supplemental Tables 1 and 2).

Development of human mast cells in hSCF Tg NSG recipients

We next investigated the development of human mast cells in the membrane-bound hSCF-expressing NSG mice. Overall, the frequencies of $cKit^+CD203c^+$ cells within total BM $CD33^+$ myeloid cells were similar between hSCF Tg NSG and non-Tg NSG recipients when excluding 2 non-Tg NSG recipients observed for more than 8 months ($P = .1439$ by 2-tailed t test; Figure 2D; Table 1). In 7 of 20 hSCF Tg NSG recipients, compared with one of 10 non-Tg NSG recipients, the frequency of $cKit^+CD203c^+$ cells in BM $CD33^+$ cells was greater than 15% (Figure 2D; Table 1). When these $cKit^+CD203c^+$ cells were FACS-purified and examined by MGG staining, their morphology was consistent with mast cells with various degrees of cytoplasmic granulation (Figure 3A-B). Histologic examination of H&E-stained bone sections showed increased cellularity in hSCF Tg NSG recipients compared with non-Tg NSG recipients (Figure 3C). We then performed IHC staining for mast cell tryptase to identify human mast cells in the BM. Consistent with the quantitative analysis by flow cytometry, $tryptase^+$ cells were abundantly observed in the hSCF Tg NSG recipients compared with non-Tg NSG recipients (Figure 3C). This does not reflect an increase in mouse mast cells because nearly all nucleated hematopoietic cells in the hSCF Tg NSG recipients are of human origin (Figure 1D). The same sections were further subjected to the immunofluorescence staining followed by confocal imaging demonstrating that these are mast cells and not $CD14^+$ monocytes (supplemental Figure 4).

Mast cell progenitors and mature mast cells reside in high frequencies in the spleen of normal immunocompetent mice.[21] We next examined the spleen of human HSC-engrafted hSCF Tg NSG recipients. Human $CD33^{high}$c-$Kit^+CD203c^+$ mast cells accounted for the highest frequency among total $hCD45^+hCD33^+$ myeloid cells in the spleen of both hSCF Tg NSG and non-Tg NSG HSC-engrafted recipients (Figure 4A-B). However, the frequencies of human mast cells in the myeloid cell population were significantly higher in hSCF Tg NSG recipients than in non-Tg NSG controls (hSCF Tg: 77.4% ± 4.5%; n = 20 and non-Tg NSG controls: 62.5% ± 3.9%; n = 12; $P = .0304$ by 2-tailed t test; Figure 4B). These human cells with surface expression phenotype of mast cells also showed morphologic features of mature mast cells (Figure 4C). Mast cell tryptase IHC staining confirmed the presence of human mast cells within the recipient spleen (Figure 4D). These findings indicate that the expression of membrane-bound human SCF in the recipient mouse microenvironment enhances development of human mast cells from transplanted human HSCs within hematopoietic organs, such as the BM and spleen, consistent with the activation of c-Kit signaling.

Next, we investigated whether the transgenic expression of hSCF results in the efficient development of mucosal tissue-type human mast cells in respiratory and gastrointestinal mucosal layers, as well as in hematopoietic organs. For this purpose, we performed IHC staining of human tryptase-expressing mast cells in the lung, stomach, small intestine, and large intestine in hSCF Tg NSG and non-Tg NSG recipients. In the hSCF Tg NSG recipient lungs, human tryptase-positive mast cells were identified within cellular infiltrates (supplemental Figure 5). In tissue sections from the stomach, small intestine, and large intestine, human tryptase-positive mast cells were present in both hSCF Tg NSG and non-Tg NSG recipients (Figure 5A-B). The mast cell $tryptase^+$ cells in gastrointestinal tissues of hSCF Tg mice were further examined by immunofluorescence microscopy using anti–human CD45 and anti–human-c-Kit antibodies. We found the presence of $hCD45^+$c-Kit^+ cells in the gastric tissues of the hSCF Tg recipients consistent with IHC staining for mast cell tryptase (Figure 5C). Because gastric tissue is one of the major sites of mast cell populations in humans and mice, we quantified human mast cells in the gastric tissue of hSCF Tg and non-Tg NSG recipients transplanted with human HSCs. IHC staining for human mast cell tryptase followed by quantification of $tryptase^+$ cells demonstrated the presence of human mast cells in gastric tissues of hSCF Tg NSG recipients (7.01% ± 0.63%, 3 sites per recipient analyzed in 3 mice) compared with non-Tg NSG recipients (2.53% ± 0.53%, 3 sites per recipient analyzed in 3 mice; $P < .0001$ by 2-tailed t test; Figure 5D). Collectively, transgenic expression of human membrane-bound SCF influences human myeloid development and mast cell development in hematopoietic organs and mucosal tissues along with the achievement of high chimerism of human hematopoietic cells in hematopoietic organs.

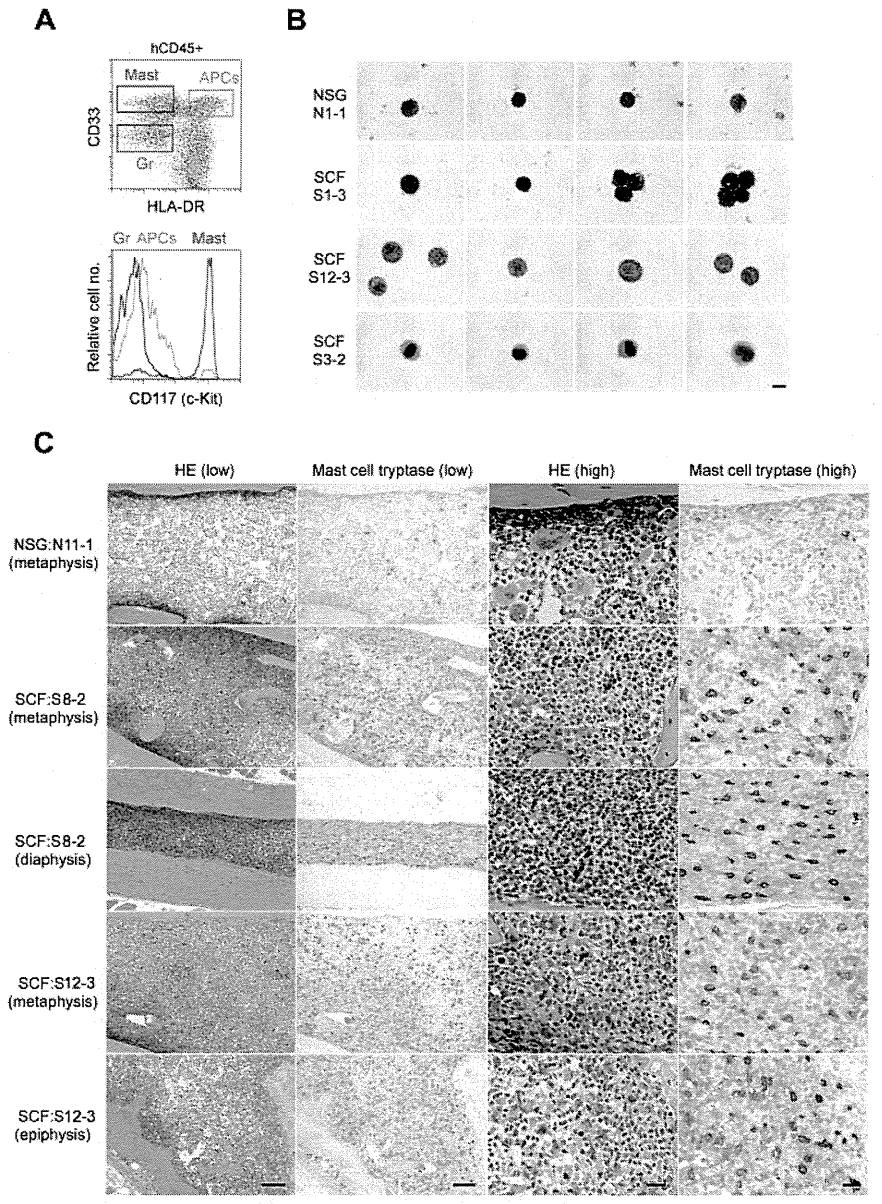

Figure 3. Human mast cell development in hSCF Tg NSG recipient BM. (A) Representative flow cytometric scatter plot and histogram demonstrating the identification of human $CD45^+CD33^+CD117^+$ mast cells. (B) FACS-sorted $hCD45^+CD33^+CD117^+CD203c^+$ human mast cells from a representative non-Tg NSG recipient BM (N1-1, 0.9% human mast cells within $hCD45^+CD33^+$ population) and hSCF Tg NSG recipient BM (S1-3, 14.6%; S12-3, 8.8%; and S3-2, 7.3% human mast cells within the $hCD45^+CD33^+$ population) were examined by MGG staining (N1-1, killed at 21 weeks; S1-3, killed at 21 weeks; S12-3, killed at 13 weeks; and S3-2, killed at 15 weeks). (C) H&E- and anti-mast cell tryptase antibody–stained bone sections demonstrate hypercellular BM with high frequency of $tryptase^+$ human mast cells in hSCF Tg NSG recipients. Non-Tg NSG recipient: N11-1, 70.7% $hCD45^+$. hSCF Tg NSG recipients: S8-2, 99.6%; and S12-3, 79.5% $hCD45^+$ (N11-1, killed at 20 weeks; S8-2, killed at 11 weeks; and S12-3, killed at 13 weeks).

Discussion

A supportive microenvironment is essential for hematopoietic and immune system homeostasis. Critical roles played by various niches in the maintenance of cell cycle quiescence and self-renewal capacity of HSCs have been demonstrated, and the thymic microenvironment is critical for T-cell education.[22,23] However, despite significant progress over the last decade, the stromal microenvironment within the humanized mouse is predominately of mouse origin. Although several key molecules, such as SDF1, are cross-reactive between human and mouse, a humanized microenvironment is required both to further improve human hematopoietic development in the recipients and to investigate in vivo the interactions between hematopoietic cells and their microenvironment.

In the present study, we humanized membrane-bound stem cell factor [SCF = KIT ligand (KL)] using the construct and mouse strain created by Majumdar et al.[13] Toksoz et al reported that human membrane-bound SCF expressed by mouse stromal cells efficiently supports long-term human hematopoiesis in vitro.[24] The importance of SCF interaction with $cKit^+$ HSCs and mast cell progenitors in murine hematopoiesis is highlighted by the hematopoietic abnormalities in mice with *Kitl* and *Kit* mutations.[25-27] In human hematopoiesis, SCF-cKit signaling is critical for the maintenance of stem and progenitor cell activities.[28] Human SCF/KL has been shown to drive cell-cycle entry by primitive hematopoietic cells in vitro.[29] Both long-term colony-initiation and colony-forming capacities are expanded ex vivo by cytokine supplementation that includes SCF/KL.[30-32] Therefore, to elucidate the role of membrane-bound human SCF in differentiation, proliferation, and maturation of human hematopoiesis in vivo, we created a novel NSG mouse strain that can support the engraftment of human HSCs and express hSCF in microenvironment. In hSCF Tg NSG recipients transplanted with human HSCs, the engraftment levels of human $CD45^+$ cells were significantly higher compared with non-Tg NSG controls. Majumdar et al reported that human SCF binds mouse c-Kit receptor but that the binding affinity is

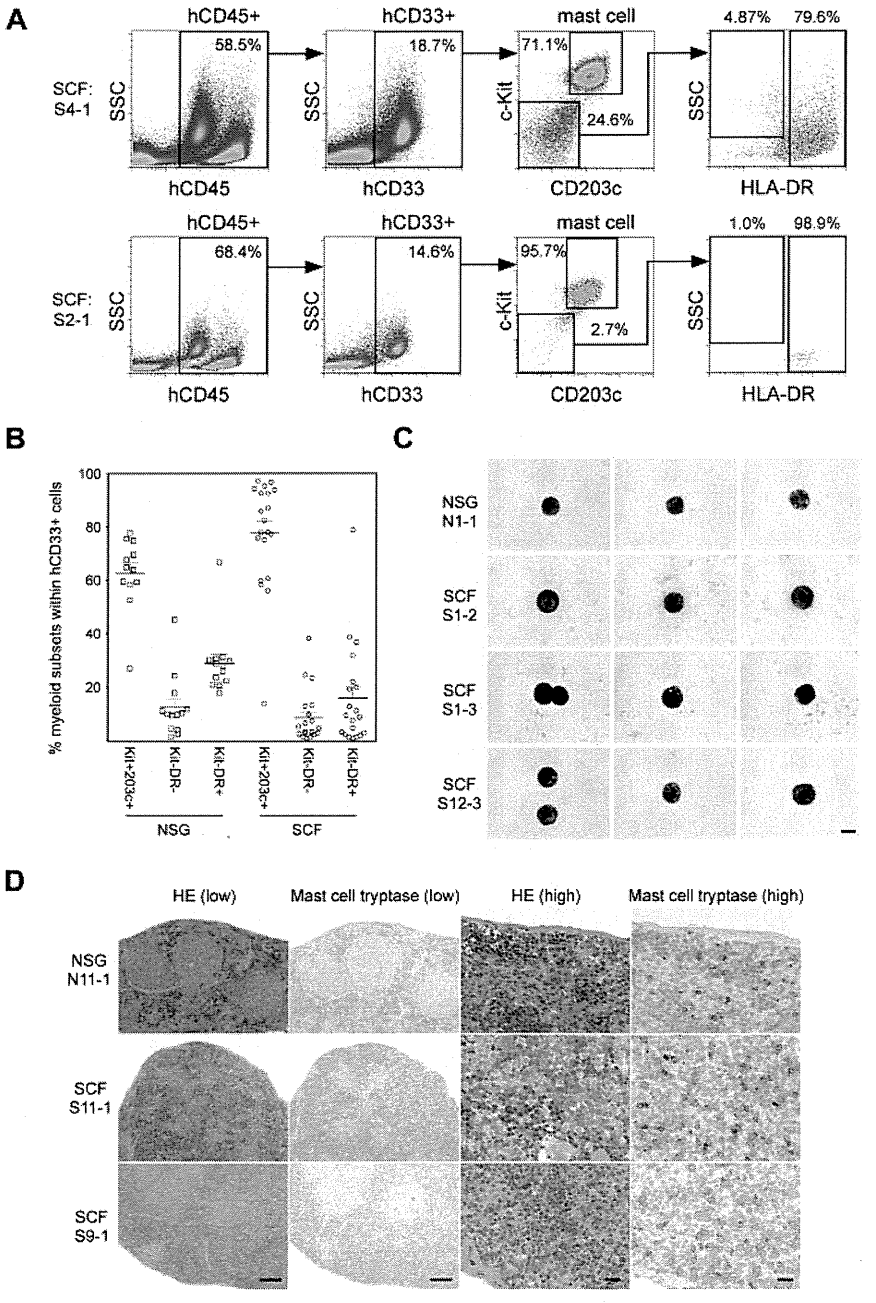

Figure 4. Human mast cell development in hSCF Tg NSG recipient spleen. (A) Human mast cell development is enhanced in hSCF Tg NSG recipient spleens (S4-1, killed at 13 weeks; and S2-1, killed at 16 weeks). (B) Frequencies of human c-Kit$^+$CD203c$^+$ mast cells, CD33$^+$HLA-DR$^-$ granulocyte population, and CD33$^+$HLA-DR$^+$ APCs within total hCD45$^+$hCD33$^+$ myeloid cells in the spleens of hSCF Tg and non-Tg NSG recipients. Human mast cell development in the spleen was significantly greater in the hSCF Tg NSG recipients (hSCF Tg: n = 20, non-Tg NSG: n = 12, $P = .0304$). (C) FACS-sorted hCD45$^+$CD33$^+$CD117$^+$CD203c$^+$ human mast cells from a representative non-Tg NSG recipient spleen (N1-1, 59.3% human mast cells within hCD45$^+$CD33$^+$ population) and hSCF Tg NSG recipient spleen (S1-2, 85.7%; S1-3, 77.7%; and S12-3, 56.1% human mast cells within hCD45$^+$CD33$^+$ population) were examined by MGG staining (N1-1, killed at 21 weeks; S1-2, killed at 20 weeks; S1-3, killed at 21 weeks; and S12-3, killed at 13 weeks). (D) H&E- and anti–mast cell tryptase antibody–stained spleen sections demonstrating the presence of human mast cells in non-Tg NSG recipients and hSCF Tg NSG recipients (non-Tg NSG recipient: N11-1, 94.0% hCD45$^+$; hSCF Tg NSG recipients: S11-1, 95.3%; and S9-1, 97.0% hCD45$^+$; N11-1, killed at 20 weeks; S11-1, killed at 10 weeks; and S9-1, killed at 16 weeks).

weaker compared with the binding affinity of human SCF to human c-Kit.[13] Therefore, the significant improvement of human hematopoietic chimerism could be attributed to preferential binding of human SCF to human HSCs instead of murine c-Kit$^+$ HSCs resulting in accelerated signaling through c-Kit in human HSCs and by impaired or attenuated support of mouse HSCs.[1,33,34] Presumably because of the competition between human and mouse hematopoietic stem or myeloid/erythroid progenitor cells, we observed diminished mouse erythrocyte hemoglobin concentration with normal range of mean corpuscular volume, mean corpuscular hemoglobin, and mean corpuscular hemoglobin concentration in all the 21 hSCF Tg NSG recipients but not in any of the non-Tg NSG recipients or nontransplanted hSCF Tg NSG adults. In addition to the greatly increased levels of human hematopoietic repopulation, we identified significant differences in human hematopoietic differentiation in hSCF Tg NSG recipients compared with non-Tg NSG recipients. Namely, there were substantially increased levels of human myeloid differentiation from HSCs in the hSCF Tg NSG mice, whereas human B cells accounted for the greatest population in the BM of non-Tg NSG mice. Because normal human BM contains myeloid cells at a relatively high frequency (36.2%-62.2%),[35] human SCF may be important in recapitulating human BM myelopoiesis in immunodeficient mice. In addition, membrane-bound human SCF may exert distinct effects on human myeloid development in the BM and in the spleen. In the BM of hSCF Tg recipients, the majority of human myeloid cells were c-Kit$^-$CD203c$^-$HLA-DR$^-$ granulocytes. Among these granulocytes, myeloid cells at various levels of maturity were identified, with myelocytes and metamyelocytes predominating in the majority of hSCF Tg NSG recipients. Because immature cells were more prominent in hSCF Tg NSG recipients compared with non-Tg NSG recipients, we performed microarray analysis to

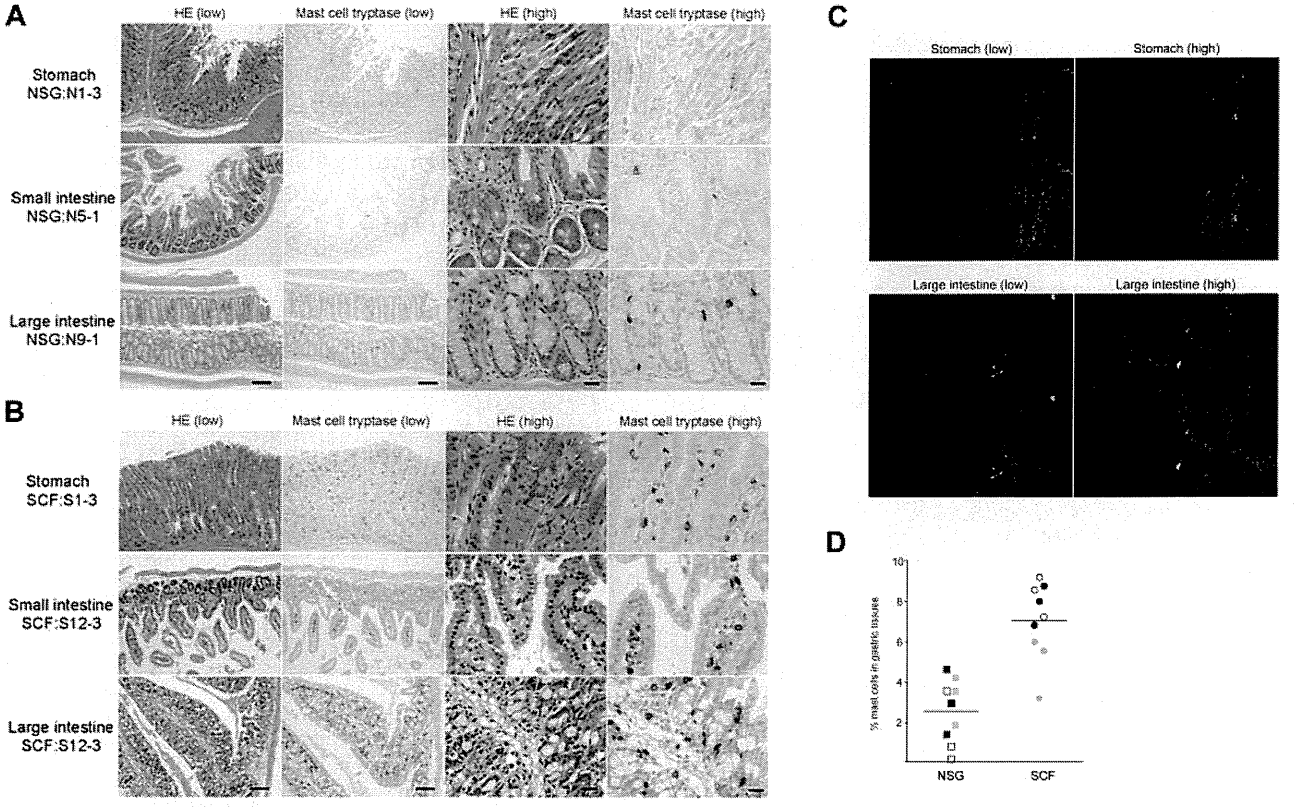

Figure 5. Human mast cell development in hSCF Tg NSG recipient stomach, small intestine, and large intestine. H&E- and anti–mast cell tryptase antibody–stained sections of (A) non-Tg NSG recipient stomach (NSG control, N1-3), small intestine (N5-1), and large intestine (N9-1) and (B) hSCF Tg NSG recipient stomach (S1-3), small intestine (S12-3), and large intestine (S12-3) demonstrating the presence of human mast cells (N1-3, killed at 24 weeks; N5-1, killed at 35 weeks; N9-1, killed at 20 weeks; S1-3, killed at 21 weeks; and S12-3, killed at 13 weeks). (C) Confocal immunofluorescence images of hSCF Tg stomach (S1-9) demonstrate human CD45$^+$ (green) and human CD117$^+$ (red) mast cells. (D) Frequencies of tryptase$^+$ cells were quantified by sampling 3 areas each from hSCF Tg (n = 3) and non-Tg (n = 3) NSG recipients: hSCF Tg NSG recipients, 7.0% ± 0.6%; and non-Tg NSG recipients, 2.5% ± 0.5% ($P < .0001$ by 2-tailed t test).

identify transcriptional signature specific to the immature human granulocytes that developed in the hSCF Tg NSG mice. Approximately 300 genes were differentially transcribed in the immature granulocytes in hSCF Tg NSG recipients compared with the mature granulocytes in non-Tg NSG recipients. Some of the up-regulated genes were associated with cell cycle or metabolism.

In several hSCF Tg NSG recipients, human mast cells composed the greatest subfraction among engrafted human myeloid cells. In the spleens of hSCF Tg NSG-engrafted mice, human mast cells were present at the highest frequency among the myeloid lineage developed in the recipients. MGG staining revealed both mature and immature mast cells in hSCF Tg NSG recipient BM. Human mast cells were identified not only in hematopoietic organs but also in lung, gastric tissue, and intestinal tissues of hSCF Tg NSG recipients. Aberrant expression of CD30 and CD25 on mast cells is associated with systemic mastocytosis and other mast cell disorders.[36,37] We did not find significantly up-regulated expression of these antigens in the mast cells derived from BM or spleen of hSCF Tg NSG recipients.

To date, several mouse strains have been developed for supporting normal and malignant human hematopoietic cell engraftment and normal myeloid cell differentiation using *Il2rg*^{null} immune-compromised mice (supplemental Table 3).[5,6,8,9,20,38-41] Among these, human thrombopoietin knock-in *Rag2*^{null} *Il2rg*^{null} mice were reported to support both human hematopoietic engraftment and myeloid differentiation in the BM. Both SCF and thrombopoietin exhibit species specificity between humans and mouse in supporting HSCs and myeloid cells in both species. These approaches focusing on the 2 distinct molecules based on the 2 immune-compromised mouse backgrounds will allow us to investigate human hematopoiesis and immunity from stem cells to myeloid progenitors to mature myeloid effecter cells in vivo. Altogether, the newly created hSCF Tg NSG mouse model engrafted with purified human HSCs will facilitate the in vivo understanding of human hematopoietic hierarchy and mast cell biology.

Acknowledgments

The authors thank David Williams for providing C3H/HeJ mice carrying the human SCF transgene and Dr Kodo and his staff at the Tokyo Cord Blood Bank for their generous assistance in processing and providing cord blood samples.

This work was supported by the National Institutes of Health (research grants HL077642, CA34196, AI46629, UO1 AI073871, DK089572), the University of Massachusetts Center for AIDS Research (P30 AI042845), the Juvenile Diabetes Foundation, International, the Helmsley Foundation, USAMRIID (L.D.S.), Project for Developing Innovation Systems, Program for Fostering Regional Innovation (O.O.), Takeda Science Foundation and Ministry of Education, Culture, Sports, Science and Technology, Japan (F.I.), and the Japan Society for the Promotion of Science through the Funding Program for Next Generation World-Leading Researchers (NEXT Program), initiated by the Council for Science and Technology Policy.

The contents of this publication are solely the responsibility of the authors and do not necessarily represent the official views of the National Institutes of Health.

Authorship

Contribution: S. Takagi, S. Tanaka, T.H., and S.M. performed the experiments; A.H., T.W., and O.O. performed and analyzed the microarray experiments; J.K., H. Kiyono, H. Koseki, O.O., T.S., and S. Taniguchi participated in discussions on research planning and analysis of results; and S. Takagi, Y.S., L.D.S., and F.I. designed the research and wrote the paper.

Conflict-of-interest disclosure: The authors declare no competing financial interests.

Correspondence: Fumihiko Ishikawa, Research Unit for Human Disease Models, RIKEN Research Center for Allergy and Immunology, 1-7-22 Suehiro-cho Tsurumi-ku, Yokohama, Kanagawa, Japan 230-0045; e-mail: f_ishika@rcai.riken.jp.

References

1. Manz MG. Human-hemato-lymphoid-system mice: opportunities and challenges. *Immunity.* 2007;26(5):537-541.
2. Shultz LD, Ishikawa F, Greiner DL. Humanized mice in translational biomedical research. *Nat Rev Immunol.* 2007;7(2):118-130.
3. McCune JM, Namikawa R, Kaneshima H, Shultz LD, Lieberman M, Weissman IL. The SCID-hu mouse: murine model for the analysis of human hematolymphoid differentiation and function. *Science.* 1988;241(4873):1632-1639.
4. Mosier DE, Gulizia RJ, Baird SM, Wilson DB. Transfer of a functional human immune system to mice with severe combined immunodeficiency. *Nature.* 1988;335(6187):256-259.
5. Ishikawa F, Yasukawa M, Lyons B, et al. Development of functional human blood and immune systems in NOD/SCID/IL2 receptor gamma chain-(null) mice. *Blood.* 2005;106(5):1565-1573.
6. Ito M, Hiramatsu H, Kobayashi K, et al. NOD/SCID/gamma(c)(null) mouse: an excellent recipient mouse model for engraftment of human cells. *Blood.* 2002;100(9):3175-3182.
7. Shultz LD, Banuelos S, Lyons B, et al. NOD/LtSz-Rag1nullPfpnull mice: a new model system with increased levels of human peripheral leukocyte and hematopoietic stem-cell engraftment. *Transplantation.* 2003;76(7):1036-1042.
8. Shultz LD, Lyons BL, Burzenski LM, et al. Human lymphoid and myeloid cell development in NOD/LtSz-scid IL2R gamma null mice engrafted with mobilized human hemopoietic stem cells. *J Immunol.* 2005;174(10):6477-6489.
9. Traggiai E, Chicha L, Mazzucchelli L, et al. Development of a human adaptive immune system in cord blood cell-transplanted mice. *Science.* 2004; 304(5667):104-107.
10. Strowig T, Gurer C, Ploss A, et al. Priming of protective T cell responses against virus-induced tumors in mice with human immune system components. *J Exp Med.* 2009;206(6):1423-1434.
11. Jaiswal S, Pearson T, Friberg H, et al. Dengue virus infection and virus-specific HLA-A2 restricted immune responses in humanized NOD-scid IL2rgammanull mice. *PLoS One.* 2009;4(10): e7251.
12. Shultz LD, Saito Y, Najima Y, et al. Generation of functional human T-cell subsets with HLA-restricted immune responses in HLA class I expressing NOD/SCID/IL2r gamma(null) humanized mice. *Proc Natl Acad Sci U S A.* 2010; 107(29):13022-13027.
13. Majumdar MK, Everett ET, Xiao X, et al. Xenogeneic expression of human stem cell factor in transgenic mice mimics codominant c-kit mutations. *Blood.* 1996;87(8):3203-3211.
14. Hong F, Breitling R, McEntee CW, et al. RankProd: a bioconductor package for detecting differentially expressed genes in meta-analysis. *Bioinformatics.* 2006;22(22):2825-2827.
15. Draghici S, Khatri P, Martins RP, et al. Global functional profiling of gene expression. *Genomics.* 2003;81(2):98-104.
16. Benjamini Y, Hochberg Y, et al. Controlling the false discovery rate: a practical and powerful approach to multiple testing. *J R Stat Soc B Met.* 1995;57(1):289-300.
17. Kawashima I, Zanjani ED, Almaida-Porada G, Flake AW, Zeng H, Ogawa M. CD34+ human marrow cells that express low levels of Kit protein are enriched for long-term marrow-engrafting cells. *Blood.* 1996;87(10):4136-4142.
18. Sakabe H, Kimura T, Zeng Z, et al. Haematopoietic action of flt3 ligand on cord blood-derived CD34-positive cells expressing different levels of flt3 or c-kit tyrosine kinase receptor: comparison with stem cell factor. *Eur J Haematol.* 1998;60(5): 297-306.
19. Yoshikubo T, Inoue T, Noguchi M, Okabe H. Differentiation and maintenance of mast cells from CD34+ human cord blood cells. *Exp Hematol.* 2006;34(3):320-329.
20. Hiramatsu H, Nishikomori R, Heike T, et al. Complete reconstitution of human lymphocytes from cord blood CD34+ cells using the NOD/SCID/gammacnull mice model. *Blood.* 2003;102(3): 873-880.
21. Arinobu Y, Iwasaki H, Gurish MF, et al. Developmental checkpoints of the basophil/mast cell lineages in adult murine hematopoiesis. *Proc Natl Acad Sci U S A.* 2005;102(50):18105-18110.
22. Kiel MJ, Morrison SJ. Uncertainty in the niches that maintain haematopoietic stem cells. *Nat Rev Immunol.* 2008;8(4):290-301.
23. Jenkinson EJ, Jenkinson WE, Rossi SW, Anderson G. The thymus and T-cell commitment: the right niche for Notch? *Nat Rev Immunol.* 2006;6(7):551-555.
24. Toksoz D, Zsebo KM, Smith KA, et al. Support of human hematopoiesis in long-term bone marrow cultures by murine stromal cells selectively expressing the membrane-bound and secreted forms of the human homolog of the steel gene product, stem cell factor. *Proc Natl Acad Sci U S A.* 1992;89(16):7350-7354.
25. Besmer P, Manova K, Duttlinger R, et al. The kit-ligand (steel factor) and its receptor c-kit/W: pleiotropic roles in gametogenesis and melanogenesis. *Dev Suppl.* 1993;125-137.
26. Geissler EN, McFarland EC, Russell ES. Analysis of pleiotropism at the dominant white-spotting (W) locus of the house mouse: a description of ten new W alleles. *Genetics.* 1981;97(2):337-361.
27. Russell ES. Hereditary anemias of the mouse: a review for geneticists. *Adv Genet.* 1979;20:357-459.
28. Broudy VC. Stem cell factor and hematopoiesis. *Blood.* 1997;90(4):1345-1364.
29. Leary AG, Zeng HQ, Clark SC, Ogawa M. Growth factor requirements for survival in G0 and entry into the cell cycle of primitive human hemopoietic progenitors. *Proc Natl Acad Sci U S A.* 1992; 89(9):4013-4017.
30. Bernstein ID, Andrews RG, Zsebo KM. Recombinant human stem cell factor enhances the formation of colonies by CD34+ and CD34+lin− cells, and the generation of colony-forming cell progeny from CD34+lin− cells cultured with interleukin-3, granulocyte colony-stimulating factor, or granulocyte-macrophage colony-stimulating factor. *Blood.* 1991;77(11):2316-2321.
31. Haylock DN, To LB, Dowse TL, Juttner CA, Simmons PJ. Ex vivo expansion and maturation of peripheral blood CD34+ cells into the myeloid lineage. *Blood.* 1992;80(6):1405-1412.
32. Petzer AL, Hogge DE, Landsdorp PM, Reid DS, Eaves CJ. Self-renewal of primitive human hematopoietic cells (long-term-culture-initiating cells) in vitro and their expansion in defined medium. *Proc Natl Acad Sci U S A.* 1996;93(4):1470-1474.
33. Lev S, Yarden Y, Givol D. Dimerization and activation of the kit receptor by monovalent and bivalent binding of the stem cell factor. *J Biol Chem.* 1992;267(22):15970-15977.
34. Martin FH, Suggs SV, Langley KE, et al. Primary structure and functional expression of rat and human stem cell factor DNAs. *Cell.* 1990;63(1):203-211.
35. Terstappen LW, Safford M, Loken MR. Flow cytometric analysis of human bone marrow: III. Neutrophil maturation. *Leukemia.* 1990;4(9):657-663.
36. Pardanani A. Systemic mastocytosis in adults: 2011 update on diagnosis, risk stratification, and management. *Am J Hematol.* 2011;86(4):362-371.
37. Sotlar K, Cerny-Reiterer S, Petat-Dutter K, et al. Aberrant expression of CD30 in neoplastic mast cells in high-grade mastocytosis. *Mod Pathol.* 2011;24(4):585-595.
38. Rongvaux A, Willinger T, Takizawa H, et al. Human thrombopoietin knockin mice efficiently support human hematopoiesis in vivo. *Proc Natl Acad Sci U S A.* 2011;108(6):2378-2383.
39. Pearson T, Shultz LD, Miller D, et al. Non-obese diabetic-recombination activating gene-1 (NOD-Rag1 null) interleukin (IL)-2 receptor common gamma chain (IL2r gamma null) null mice: a radioresistant model for human lymphohaematopoietic engraftment. *Clin Exp Immunol.* 2008;154(2): 270-284.
40. Brehm MA, Cuthbert A, Yang C, et al. Parameters for establishing humanized mouse models to study human immunity: analysis of human hematopoietic stem cell engraftment in three immunodeficient strains of mice bearing the IL2rgamma(null) mutation. *Clin Immunol.* 2010;135(1):84-98.
41. Strowig T, Rongvaux A, Rathinam C, et al. Transgenic expression of human signal regulatory protein alpha in Rag2−/−gammac−/− mice improves engraftment of human hematopoietic cells in humanized mice. *Proc Natl Acad Sci U S A.* 2011;108(32):13218-13223.